Hindawi
Mathematical Problems in Engineering
Volume 2020, Article ID 2906973, 13 pages
https://doi.org/10.1155/2020/2906973

Research Article

Simulation Model of Bottom Hole Dynamic Pressure and Reservoir Dynamic Stress in Hydraulic Fracturing with Pulse Injection

Ge Zhu and Shimin Dong

School of Mechanical Engineering, Yanshan University, Qinhuangdao, Hebei, 066004, China

Correspondence should be addressed to Shimin Dong; ysudshm@ysu.edu.cn

Received 12 August 2020; Revised 27 September 2020; Accepted 29 September 2020; Published 20 October 2020

Academic Editor: Ivan Giorgio

To study the mechanism of hydraulic fracturing with pulse injection theoretically, in this paper, the transient flow model of fracturing fluid in the pipe string was established, and it was solved by method of characteristics and finite difference method, respectively. Furthermore, the elastodynamic model of reservoir was also established. Based on the finite element method, the dynamic stress distribution in the reservoir was simulated and calculated. In addition, the influence of parameters in the pulse injection scheme on dynamic stress was analyzed. The results indicate that the unsteady injection produces a pulse pressure wave at the wellhead. The pressure wave propagates along the pipe string to the bottom of the well, and its amplitude attenuates due to the resistance loss. When the pressure wave propagates to the bottom of the well, it will be reflected and there is a superposition area of the downward pressure wave and upward reflection wave near the bottom hole. The bottom hole pressure of pulse injection is the sum of stable injection pressure and the above pressure wave. Simultaneously, this fluid pressure with pulse variation will stimulate reservoir to produce dynamic stress in its interior. The pulse adjustment time and adjustment amplitude in the injection scheme have a significant impact on the dynamic stress. The results of this paper are helpful to understand the mechanism of hydraulic fracturing with pulse fluid injection and provide guidance for its parameter design.

1. Introduction

Hydraulic fracturing has been widely used in the reservoir stimulation, which also plays an important role in the exploitation of low permeability reservoirs and the development of geothermal energy resources [1, 2]. During hydraulic fracturing, considering the pressure bearing capacity of surface equipment and the safety of the operator, it is necessary to set safety pressure at wellhead [3, 4]. The safety pressure limits the continuous increase of wellhead pressure. Once the wellhead pressure is close to the safe pressure, the injection should be stopped even if the breakdown pressure of the reservoir is not reached. As a result, the fracturing operation is interrupted, stimulation effect is affected, and operation time and cost are increased. To solve the above problems, the pulse injection scheme by alternately stopping and starting the fracturing pumps is proposed in the field operation. This attempt has achieved considerable results in practical application. However, there is still a lack of research on its mechanism and theoretical guidance in the application.

Currently, conventional hydraulic fracturing is used more frequently. In this process, the fracturing pump usually runs at a constant speed, and the fluid injection is basically stable. In recent years, the research about unstable injection has gradually attracted extensive attention. However, it is mainly concentrated in the laboratory or industrial test. Based on the true triaxial hydraulic fracturing test system, Zhuang et al. [5, 6] conducted a test on granite samples from enhanced geothermal systems. The pressure variation, acoustic emission amplitude, and fracture morphology in different injection schemes were compared. The results show that unstable injection can increase the complexity of fractures and reduce the breakdown pressure. The above conclusions were also demonstrated by the test of Patel et al.

[7] on the sandstone specimens, Zhou et al. [8] on the artificial concrete blocks, and Hou et al. [9] on the shale specimens. Besides, the results of the laboratory test indicated that pulse injection can improve the porosity of coal samples and promote the development of microcracks [10, 11]. Due to the limitation of indoor space, the test pipe string is short. It is impossible to simulate the dynamic pressure propagation in the pipe string from hundreds to thousands of meters in practical application. Through the field test of the shale gas well, Jordan et al. [12] demonstrated that the unstable injection scheme by changing the speed of the pump can significantly increase shale gas production. Simultaneously, for coalbed methane reservoir, the field application results also showed that the injection scheme with sinusoidal variation can greatly improve the gas drainage efficiency [13, 14]. However, owing to the complex environment in the field, it is difficult to control the test factors, the monitoring means are limited, and the cost is expensive. In contrast, there are few theoretical research studies on hydraulic fracturing with unstable injection. The stress distribution in the two-dimensional model under unstable excitation was studied by Lu et al. [15] and Yoon et al. [16], through finite difference method and discrete element method, respectively. The results demonstrated that unstable injection can improve the fracturing effect. However, the above study only considered the reservoir and ignored the flow of fracturing fluid along the string. Tong et al. [17] established the mathematical model of unsteady fluid flow in wellbore, but it did not consider the influence of fluid compressibility and friction.

The essence of unstable injection is to make the fluid flow dynamically in the pipe string by adjusting the injection rate and obtain fluctuating fluid pressure at the bottom hole. Subsequently, the unstable pressure stimulates the reservoir and produces dynamic stress in it. The dynamic stress is conducive to rupture the reservoir and creates complex crack network. In the field application, the reservoir is usually located hundreds of meters or even thousands of meters underground. Whether the fluid can produce dynamic pressure at the bottom hole after passing through the long string is directly related to the engineering application of unstable injection. In summary, the above problems still need to be proved theoretically.

In this study, the transient flow model of fluid in the pipe string and the elastodynamic model of reservoir were established, respectively. Furthermore, the pressure propagation characteristics along the pipe string and the dynamic stress distribution in the reservoir were also analyzed. Finally, the influence of parameters in the pulse injection scheme was discussed. The results are helpful to provide theoretical guidance for the engineering application of pulse injection.

2. Operation Steps and Principle of Pulse Fluid Injection

2.1. Application Background. During conventional hydraulic fracturing, fluid injection is usually stable. Due to the low permeability of the reservoir, the seepage velocity at bottom hole is much lower than the injection velocity at the wellhead. With the continuous injection of fluid, the pressure in the pipe string gradually increases. The variation of wellhead pressure and bottom hole pressure is shown in Figure 1. Considering the safety of the operator and the pressure bearing capacity of the equipment, it is necessary to set the safety pressure at the wellhead. As shown in Figure 1, P_s is the safety pressure and P_f is the breakdown pressure of the reservoir. When the continuous injection time is t_2, the wellhead pressure is close to the safety pressure, while the bottom hole pressure does not reach the breakdown pressure. At this time, it is necessary to stop the injection immediately. If injection is continued, the wellhead pressure will exceed the safety pressure limit and pose a threat to the equipment and operators. Traditional treatment measures may need to adjust the fracturing process or acidify the reservoir [18]. As a result, the fracturing operation is interrupted, stimulation effect is affected, and operation time and cost are increased.

2.2. Operation Steps. Hydraulic fracturing with pulse injection overturns the conventional stable injection mode, which can effectively solve the problem of interruption caused by pressure limitation. The operation steps of pulse injection are shown in Figure 2(a), mainly including the following steps:

(1) First of all, hydraulic fracturing is carried out according to the conventional stable fluid-injection scheme. When the wellhead pressure is close to the safe pressure but the reservoir is still not ruptured, it is necessary to immediately stop the injection and confirm the stop time t_2. Subsequently, the fracturing pump is stopped to relieve the pressure. In addition, the wellhead pressure is reduced to p_0, which provides sufficient adjustment space for pulse fluid injection.

(2) Design a pulse injection scheme. As shown in Figure 2(b), first the flow rate Q_0 is used for injection. After continuous injection of t_1 time, the injection flow rate is suddenly reduced by ΔQ_j and it is maintained for Δt_j time. Subsequently, the injection flow rate is immediately increased $(\Delta Q_j + \Delta Q_s)$ and maintained for Δt_s time. Finally, the injection flow rate is restored to Q_0 and the injection continues. Certainly, the pulse adjustment must be carried out before t_2 time. The fracturing operation is conducted again according to the pulse injection scheme.

(3) Monitor the wellhead pressure variation during the entire injection process. Determine whether the wellhead pressure continues to rise and is close to the safe pressure after pulse adjustment. If the wellhead pressure does not continue to rise, it indicates that the pulse fluid-injection operation has effectively broken the reservoir. On the contrary, (1) and (2) need to be repeated until the reservoir is fractured and the wellhead pressure does not continue to rise.

2.3. Principle. The pulse adjustment of the injection rate causes transient fluctuations of fluid in the pipe string. Simultaneously, pressure fluctuations propagate along the pipe string in the form

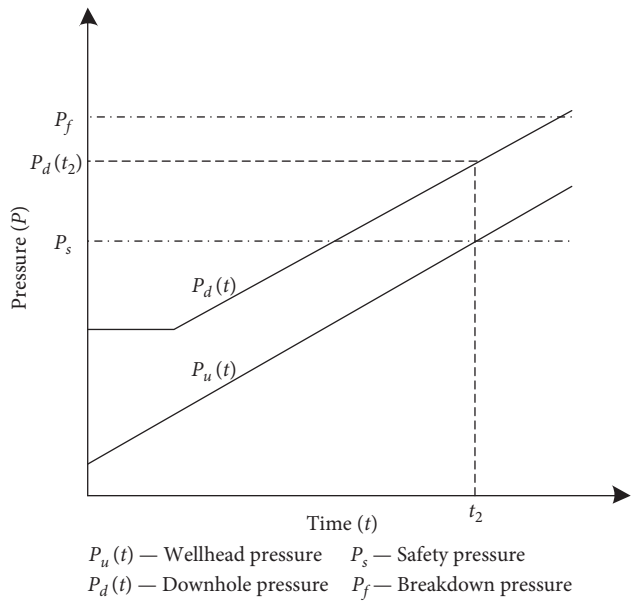

Figure 1: Pressure variation in the pipe string of conventional stable fluid injection.

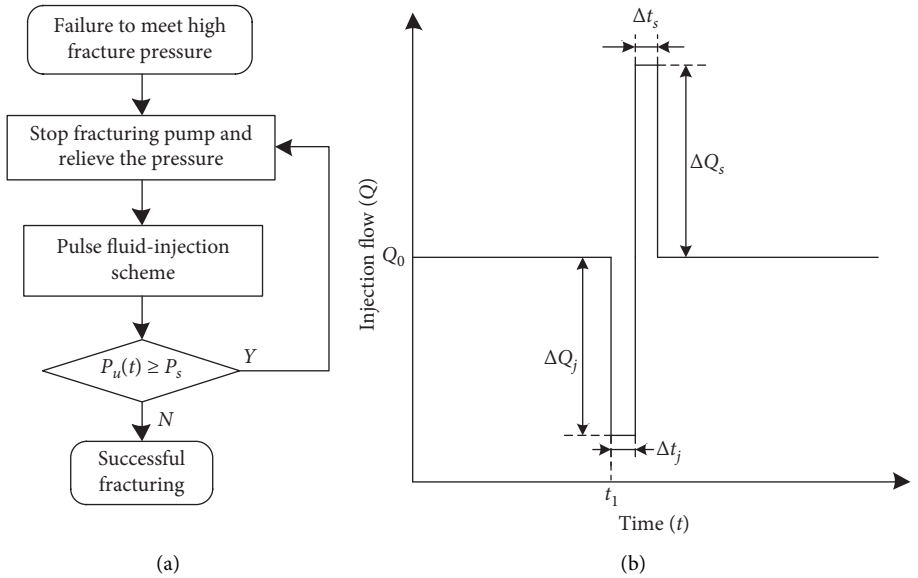

Figure 2: Main operation steps and injection schemes of pulse hydraulic fracturing. (a) Pulse fluid-injection fracturing steps. (b) Pulse fluid-injection scheme.

of pressure waves. Under the premise of ensuring that the wellhead pressure does not exceed the safety pressure limit, the pressure wave can effectively increase the bottom hole pressure. Furthermore, the pulse pressure stimulates the reservoir and creates dynamic stress inside it. The dynamic stress distribution in the reservoir has a significant effect on the initiation and propagation of fractures. To theoretically prove the principle of pulse injection, the transient dynamic model of fluid in the string and the elastic dynamic model of reservoir will be established, respectively, in the following section.

3. Dynamic Model of Transient Flow of Fracturing Fluid

To facilitate modeling, make the following assumptions: (1) Since the diameter of the pipe string is much smaller than the length, only one-dimensional flow of fracturing fluid along the length of the pipe string is considered. (2) For vertical wellbore, the axis of the pipe string is vertical. (3) The flow of fracturing fluid along the pipe string is an adiabatic process without heat exchange with the outside.

3.1. Governing Equation. For the control unit shown in Figure 3, the continuity equation is obtained by mass conservation:

$$\rho_l c^2 \frac{\partial v}{\partial z} + \frac{\partial p}{\partial t} + v\frac{\partial p}{\partial z} = 0, \tag{1}$$

where

$$c = \frac{\sqrt{(K/\rho_l)}}{\sqrt{1 + (K\,D/E_0 e)}}, \tag{2}$$

$$\rho_l = \rho_0 e^{(1/K)(p - p_0)}, \tag{3}$$

where ρ_l is the density of fracturing fluid, z is the displacement along the axis of the string, v is the velocity along the axis of the string, p is the fluid pressure, c is the propagation velocity of pressure wave, K is the elastic modulus of fracturing fluid, E_0 is the elastic modulus of the string, e is the wall thickness of the string, D is the inner wall diameter of the string, p_0 is the initial pressure at the wellhead, and ρ_0 is the density of fracturing fluid under the pressure of p_0.

The equation of motion can be obtained from the momentum theorem:

$$\frac{\partial v}{\partial t} + v\frac{\partial v}{\partial z} + \frac{1}{\rho_l}\frac{\partial p}{\partial z} + \frac{f_s v|v|}{2\,D} + J_d - g = 0, \tag{4}$$

where J_d is an unsteady friction, which takes into account the influence of transient acceleration and instantaneous convective acceleration [19, 20]:

$$J_{\mathrm{d}} = k_3\left[\frac{\partial v}{\partial t} + c \cdot \operatorname{sign}(v)\left|\frac{\partial v}{\partial z}\right|\right], \tag{5}$$

where f_s is the Darcy–Weisbach resistance coefficient, which is related to the flow state of the fluid and the roughness of the pipe wall, and k_3 is the unsteady resistance coefficient. $\operatorname{Sign}(v)$ is a symbolic function, when $v > 0$, $\operatorname{sign}(v) = 1$, and when $v < 0$, $\operatorname{sign}(v) = -1$.

The fracturing fluid is usually non-Newtonian fluid, and the resistance coefficient is calculated by the following formula [21]:

$$\frac{1}{\sqrt{\lambda}} = \left(\frac{4}{n^{0.75}} + \xi\right)\lg\left[\mathrm{Re}\lambda^{(1-(n/2))}\right] - \frac{0.4}{n^{1.2}} - 2.1\xi, \tag{6}$$

where the resistance coefficient f_s and fanning friction coefficient satisfy the following relationship:

$$f_s = 4\lambda. \tag{7}$$

The generalized Reynolds number is given by

$$\mathrm{Re} = \frac{D^n v^{2-n}\rho_l}{\gamma}, \tag{8}$$

where λ is the fanning friction coefficient, n is the rheological property index, which is determined by the experimental data, ζ is a comprehensive parameter, and γ is the rheological coefficient.

3.2. Boundary Condition

3.2.1. Injection Boundary. In the process of hydraulic fracturing with pulse fluid injection, the fracturing fluid is injected from the inlet of the pipe string. In addition, this is regarded as the velocity boundary condition of the transient flow of the fracturing fluid:

$$v|_{z=0} = \frac{4 \times Q(t)}{\pi D^2}, \tag{9}$$

where $Q(t)$ is the variable injection flow rate during the fracturing operation.

3.2.2. Reservoir Boundary. Considering that the target reservoir needs fracturing which is usually low permeability or even ultra-low permeability, the flow rate of fracturing fluid that enters the reservoir through seepage before the reservoir fracture is much less than the injection flow rate on the ground. Therefore, the velocity boundary at the exit of the downhole pipe string is simplified as follows:

$$v|_{z=L} = 0. \tag{10}$$

3.3. Initial Condition. Before hydraulic fracturing with pulse fluid injection, it is considered that the pipe string is full of fracturing fluid in static state, and the wellhead pressure is p_0:

$$\begin{cases} v|_{t=0} = 0, \\ p|_{t=0} = p_0 + \rho_l g z. \end{cases} \tag{11}$$

4. Elastodynamic Model of Reservoir

To facilitate modeling, make the following assumptions: (1) The open hole completion reservoir is simplified to a centrally symmetrical plane strain model. (2) The reservoir is homogeneous, isotropic, and linear elastic. The simplified reservoir mechanics model is shown in Figure 4.

4.1. Governing Equation. The equation of motion in polar coordinates can be expressed as follows:

$$\rho_s \frac{\partial^2 u}{\partial t^2} = \frac{\partial \sigma_r}{\partial r} + \frac{\sigma_r - \sigma_\theta}{r}, \tag{12}$$

where

$$\sigma_r = \lambda(\varepsilon_r + \varepsilon_\theta) + 2G\varepsilon_r, \tag{13}$$

$$\sigma_\theta = \lambda(\varepsilon_r + \varepsilon_\theta) + 2G\varepsilon_\theta. \tag{14}$$

The relationship between strain and displacement can be expressed as follows:

$$\begin{aligned} \varepsilon_r &= \frac{\mathrm{d}u}{\mathrm{d}r}, \\ \varepsilon_\theta &= \frac{u}{r}, \end{aligned} \tag{15}$$

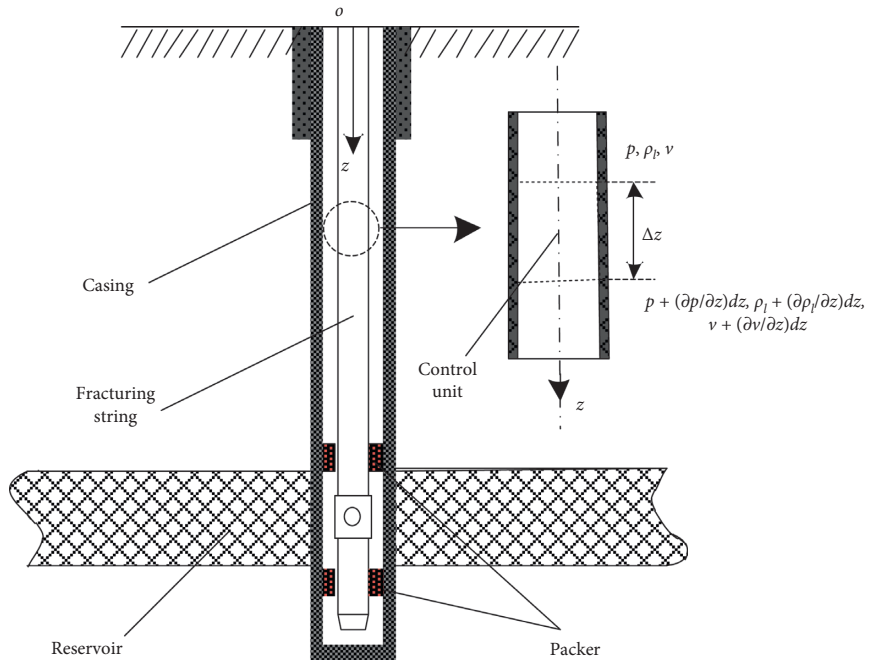

Figure 3: Schematic diagram of the fracturing pipe string and its internal fluid.

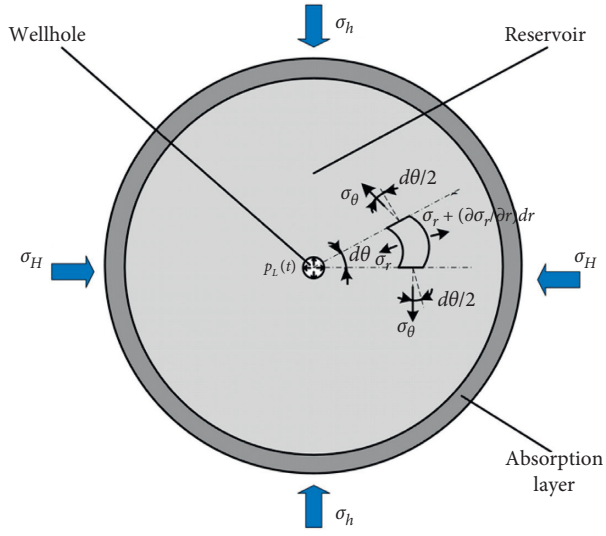

Figure 4: Plane strain mechanical model of reservoir.

where ρ_s is the rock density, σ_r is the radial stress, σ_θ is the circumferential stress, u is the radial displacement, r is the radial coordinates, and λ and G are the lame parameters.

Synthesizing equations (12)–(15), the governing equation of reservoir elastodynamics is shown as follows:

$$\frac{1}{c_s^2}\frac{\partial^2 u}{\partial t^2} = \frac{\partial^2 u}{\partial r^2} + \frac{1}{r}\frac{\partial u}{\partial r} - \frac{u}{r^2}, \tag{16}$$

where

$$c_s = \sqrt{\frac{(\lambda + 2G)}{\rho_s}} = \sqrt{\frac{E(1-\mu)}{\rho_s(1+\mu)(1-2\mu)}}, \tag{17}$$

where c_s is the propagation velocity of the elastic wave in the reservoir, E is the elastic modulus of rock, and μ is Poisson's ratio of rock.

4.2. Boundary Condition

4.2.1. Inner Boundary of Borehole. During the fracturing operation of an open hole, the fracturing fluid at the outlet of the bottom hole directly acts on the inner wall of the wellbore. Moreover, the seepage effect of reservoir is weak, and the local pressure loss caused by the sudden change of cross section can be ignored. Therefore, the internal boundary of the reservoir elastodynamic model is as follows:

$$\sigma_r = p_L(t), \tag{18}$$

where $p_L(t)$ is the bottom hole fluid pressure obtained from the transient flow dynamics model of fracturing fluid in the pipe string.

4.2.2. External Boundary. In order to simulate an infinite reservoir and eliminate the reflection of stress waves at the outer boundary under dynamic excitation, an absorbing boundary is used in the external boundary of the model. In other words, an additional absorption layer is added outside the reservoir research domain, and the stress wave is transferred from the research domain to the absorption layer and then processed by the absorption layer, without any reflection.

4.3. Initial Condition. The in situ stress near the wellbore will be redistributed after drilling, and the balanced stress field is taken as the initial condition of fracturing operation.

5. Numerical Solution and Verification

5.1. Solution and Verification of Fluid Transient Dynamic Model

5.1.1. Method of Characteristics. According to the method of characteristics [22], the partial differential equations in the abovementioned fluid transient dynamics model are converted into ordinary differential equations and integrated along the characteristic lines as shown in Figure 5. "+" represents wave propagation from upstream to downstream, while "–" represents wave propagation from downstream to upstream. The following equation is obtained:

C^+ :

$$v_p + \frac{1}{c\rho_l}P_p = v_M + \frac{1}{c\rho_l}P_M + g\,\Delta t - \frac{f_s v_M |v_M|}{2D}\Delta t - k_3\left(\frac{v_M - v_{M_0}}{\Delta t} + c\cdot \operatorname{sign}(v_M)\left|\frac{v_{P_0} - v_M}{\Delta z}\right|\right)\Delta t, \tag{19}$$

C^-:

$$v_p - \frac{1}{c\rho_l}P_p = v_N - \frac{1}{c\rho_l}P_N + g\,\Delta t - \frac{f_s v_N |v_N|}{2D}\Delta t - k_3\left(\frac{v_N - v_{N_0}}{\Delta t} + c\cdot \operatorname{sign}(v_N)\left|\frac{v_N - v_{P_0}}{\Delta z}\right|\right)\Delta t. \tag{20}$$

5.1.2. Finite Difference Method. The differential terms in the governing equation are discretized by the difference scheme as follows. S stands for pressure P or velocity v. S_i^j represents the value of j length position at time i. The difference form of time is as follows:

$$\frac{\partial S}{\partial t} = \frac{S_j^i - \left[aS_j^{i-1} + ((1-a)/2)\left(S_{j+1}^{i-1} + S_{j-1}^{i-1}\right)\right]}{\Delta t}, \tag{21}$$

where a is the weight coefficient of the difference, considering the calculation accuracy and stability factors comprehensively, and $a = 0.1$ in this paper.

The difference form of distance is as follows:

$$\frac{\partial S}{\partial z} = \frac{S_{j+1}^{i-1} - S_{j-1}^{i-1}}{2\Delta z}. \tag{22}$$

Substituting the above difference form into the fluid transient dynamics control equation, the following difference equation is obtained:

$$P_j^{i+1} = \left[-v_j^i\frac{P_{j+1}^i - P_{j-1}^i}{2\Delta z} - \rho_l c^2\frac{v_{j+1}^i - v_{j-1}^i}{2\Delta z}\right]\Delta t + \left[aP_j^i + \frac{1-a}{2}\left(P_{j+1}^i + P_{j+1}^i\right)\right], \tag{23}$$

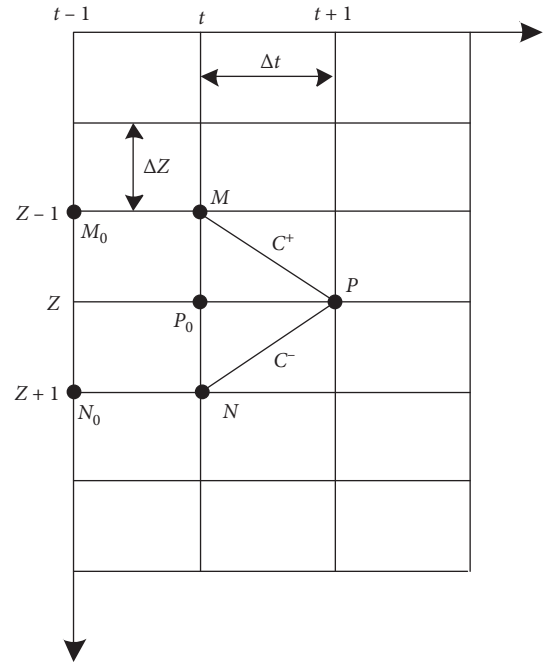

Figure 5: Time and space plane grid based on the method of characteristics.

$$v_j^{i+1} = \left[-v_j^i\frac{v_{j+1}^i - v_{j-1}^i}{2\Delta z} - \frac{1}{\rho_l}\frac{P_{j+1}^i - P_{j-1}^i}{2\Delta z} + g - \frac{f_s v_j^i |v_j^i|}{2D} - k_3\left(\frac{v_j^{i-1} - v_j^{i-2}}{\Delta t} + c\cdot \operatorname{sign}\left(v_j^{i-1}\right)\frac{v_{j+1}^{i-1} - v_{j-1}^{i-1}}{2\Delta z}\right)\right]\Delta t + \left[av_j^i + \frac{1-a}{2}\left(v_{j+1}^i + v_{j+1}^i\right)\right]. \tag{24}$$

5.1.3. Comparison of Calculation Accuracy. Considering the dynamic effect, the variation of the injection flow rate will cause fluid fluctuation in the pipe string. Therefore, in order to calculate the pressure result in the pipe string under the condition of stable fluid injection, the injection flow rate first increases linearly and then remains stable. The transient dynamic model of fluid in the pipe string is solved by the method of characteristics and the finite difference method, and the calculation results of bottom hole pressure and wellhead pressure are obtained. As shown in Figure 6, with the continuous injection of fracturing fluid, the bottom hole pressure and wellhead pressure increase approximately linearly. However, different from the traditional static theory, the bottom hole pressure does not increase immediately with the injection but needs a certain transmission time, which is determined by the length of the pipe string and the propagation velocity of the pressure wave in the fracturing fluid. By comparing the results of the two numerical methods, it is found that they are basically consistent.

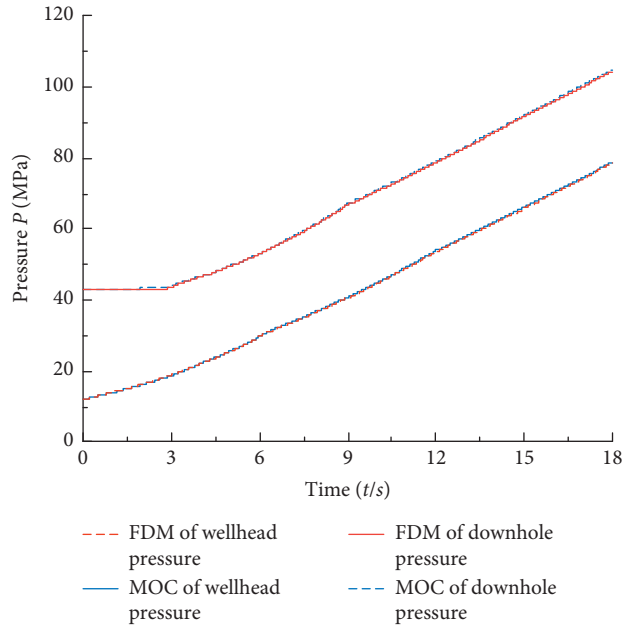

Figure 6: Comparison of calculation results of pressure in the pipe string by different numerical methods.

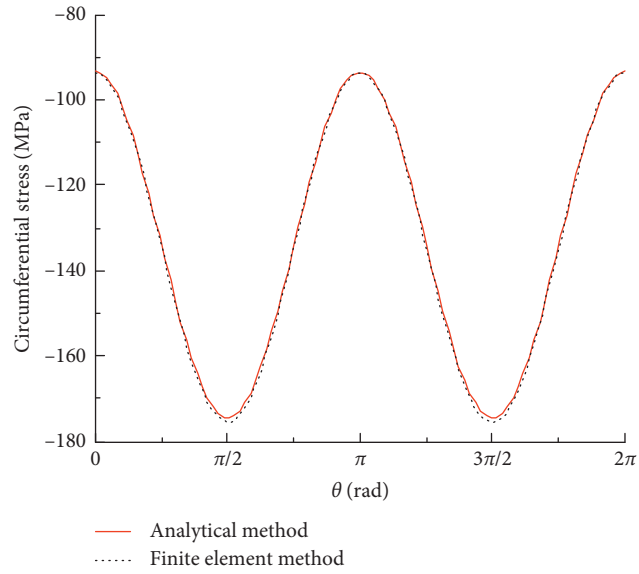

Figure 7: Comparison of circumferential stress with different methods.

5.2. Solution and Verification of Reservoir Elastodynamic Model. Based on ABAQUS software, a numerical simulation model is established to solve the problem. In the model, CPE4 element is used to simulate homogeneous and isotropic rock medium and CINPE4 infinite element is used to simulate infinite reservoirs in the absorption layer to eliminate the influence of the boundary reflected stress wave on the calculation results. The internal boundary is the bottom hole pressure at the outlet of the string calculated previously. The geostatic analysis step and implicit dynamic analysis step are set, respectively, and the stress field results calculated by the geostatic analysis step are taken as the initial conditions of the implicit dynamic analysis step.

During the verification process, the maximum horizontal principal stress σ_H is set to 79.5 MPa and the minimum horizontal principal stress σ_h is set to 57.7 MPa. Only considering the effect of in situ stress, the circumferential stress distribution in the inner wall of the wellbore is solved by the analytical method [23, 24] and the finite element method, respectively. The calculation results are shown in Figure 7. It can be seen that the circumferential stress produced by in situ stress in the inner wall of the wellbore is negative, showing compression effect, and the minimum value is in the horizontal direction and the maximum value is in the vertical direction. The results of the two methods are in good agreement.

6. Results and Discussion

In this section, the simulation will be carried out according to the operation steps of hydraulic fracturing with pulse fluid injection, and the results of transient fluid flow and reservoir dynamic response will be analyzed. Furthermore, the feasibility of the application of pulse fluid injection will be proved theoretically, and the influence of parameters in the pulse fluid-injection scheme on the fracturing effect will be discussed. The main simulation parameters involved are shown in Table 1.

6.1. Results of Pressure in Pipe String. In conventional hydraulic fracturing, fracturing fluid is injected into the pipe string according to the injection scheme shown in Figure 8(a). If a large injection flow rate is directly applied, the dynamic impact will interfere with the subsequent results, so the initial stage adopts a linear increase transition method. The pressure results shown in Figure 8(b) are obtained by simulation calculation. It can be seen that with the continuous injection of fracturing fluid, the wellhead and bottom hole pressure gradually increase. When the continuous injection time t_2 is 17.1925 s, the wellhead pressure reaches the safety pressure of 75 MPa. At this time, the bottom hole pressure is only 100.9275 MPa, which does not reach the breakdown pressure of the reservoir. If fluid injection is continued in order to increase the bottom hole pressure, it will break through the safety pressure, which will threaten the service life of the equipment and the safety of personnel. The fluid injection should be stopped immediately.

After the fracturing pump is shut down and the pressure is relieved, the pulse fluid injection is carried out according to the injection scheme shown in Figure 9(a). The pressure simulation result during the fracturing process is shown in Figure 9(b). The pulse regulation process in which the injection flow rate first decreases and then increases makes the wellhead pressure produce similar pulse variation. The pulse pressure does not exceed the safety pressure of the wellhead. Then, it propagates downhole in the form of pressure wave along the pipe string and reaches the bottom of the well at 16.7450 s. The bottom hole pressure at this time is the

Table 1: Main simulation parameters.

Parameter	Value	Unit
ρ_l	1050	kg/m^3
K	1.32	GPa
p_0	12	MPa
P_s	75	MPa
D	89	Mm
L	3000	m
r_w	0.1	m
ρ_s	2600	kg/m^3
E	30	GPa
μ	0.25	—
σ_H	79.5	MPa
σ_h	57.7	MPa

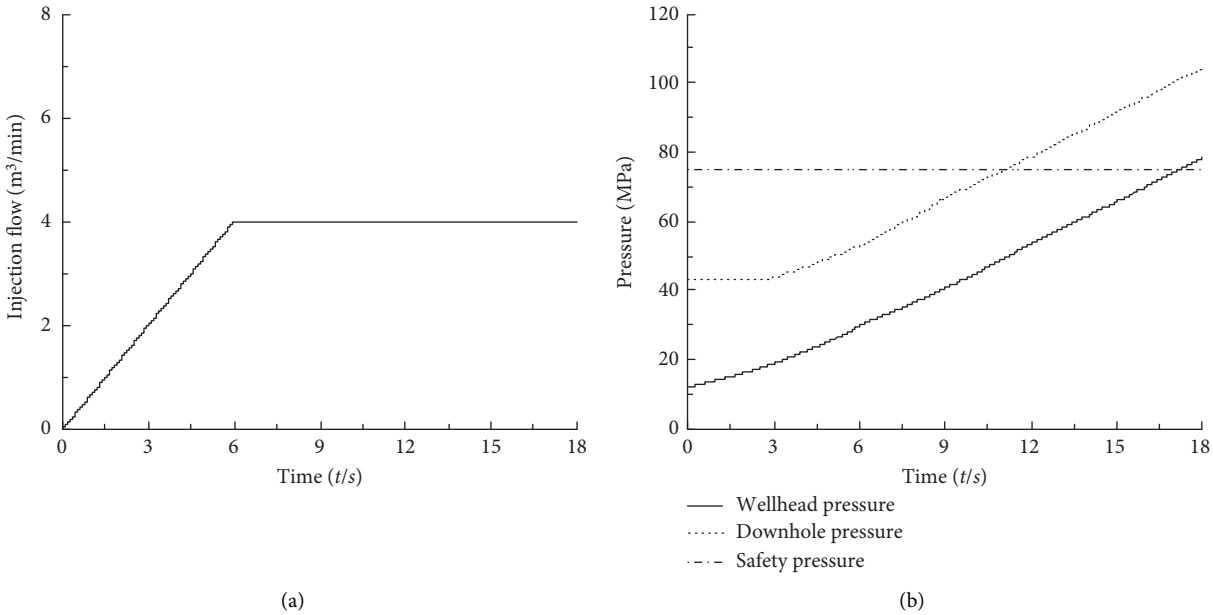

Figure 8: The conventional hydraulic fracturing stable injection scheme and the simulation results of the pressure in the pipe string. (a) Stable fluid injection scheme. (b) Variation of wellhead and downhole pressure with injection time.

superposition result of stable injection pressure and pulse pressure wave. The maximum bottom hole pressure is 108.1264 MPa, which is 7.1989 MPa higher than that of conventional stable injection.

To further analyze the propagation characteristics of the above pressure wave along the pipe string, its amplitude at different lengths of the pipe string is extracted and the results are shown in Figure 10. Due to the loss of resistance, the fluctuation amplitude generally decreases with the increase in the propagation distance. However, there is a significant increase in the range of about 250 m near the bottom of the pipe string. The analysis shows that the pressure wave will be reflected when it propagates to the bottom of the well, and the reflected wave will propagate upward in the same pattern. Thus, the downward pressure wave is superimposed with the upward pressure wave. It can be seen from Figure 10 that the amplitude of the pressure wave in the superposition range is approximately twice that of the downward pressure wave. Moreover, the peak and trough duration of the incident wave is 0.5 s. The effective superposition time after reflection is 0.25 s. From the above calculation, the propagation velocity of the pressure wave is 1048.2789 m/s. Therefore, the effective superposition area of the pressure wave is about 250 m near the bottom of the pipe string.

6.2. Results of Dynamic Stress in Reservoir. The bottom hole pressure calculated in the previous section is applied to the inner wall of wellbore as the internal boundary condition of the reservoir elastodynamic model. According to the maximum circumferential stress criterion, the circumferential stress distribution in the inner wall of wellbore has a significant influence on the location and time of hydraulic fracture initiation [23–25]. Figure 11 shows the results of circumferential stress distribution in the reservoir. It can be seen that the circumferential stress is only positive near the left and right wings of the wellbore, which shows tensile effect, while the position far away from the wellbore is mainly affected by in situ stress, showing

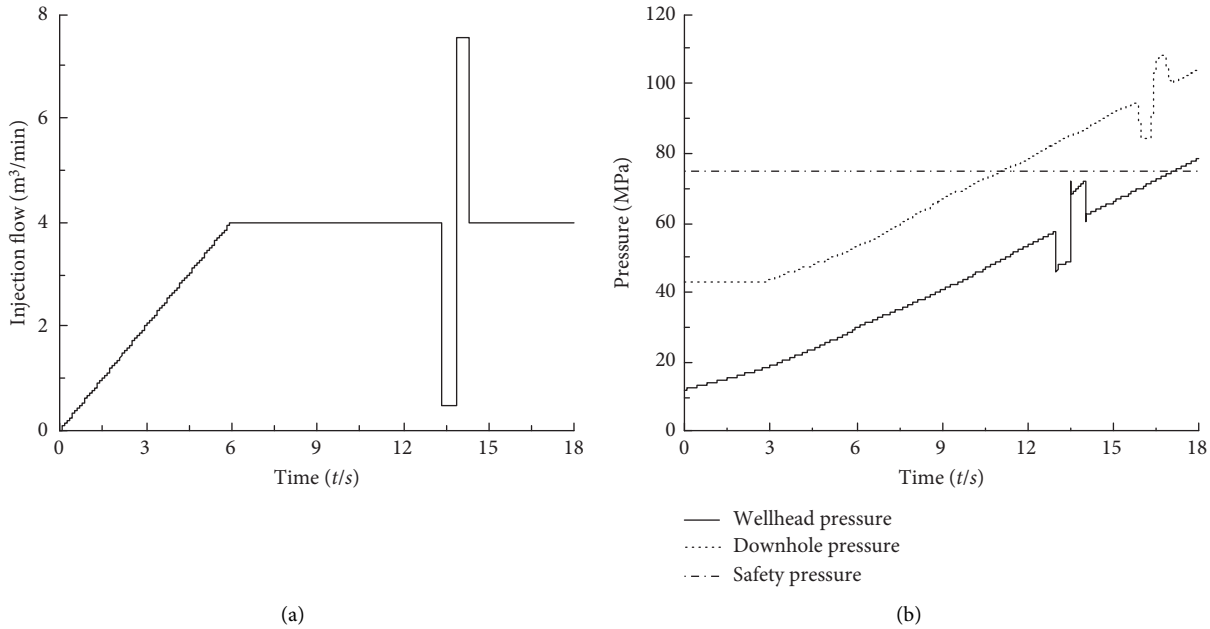

Figure 9: Pulse hydraulic fracturing fluid-injection scheme and simulation results of pressure in the string. (a) Pulse fluid-injection scheme. (b) Variation of wellhead and downhole pressure with injection time.

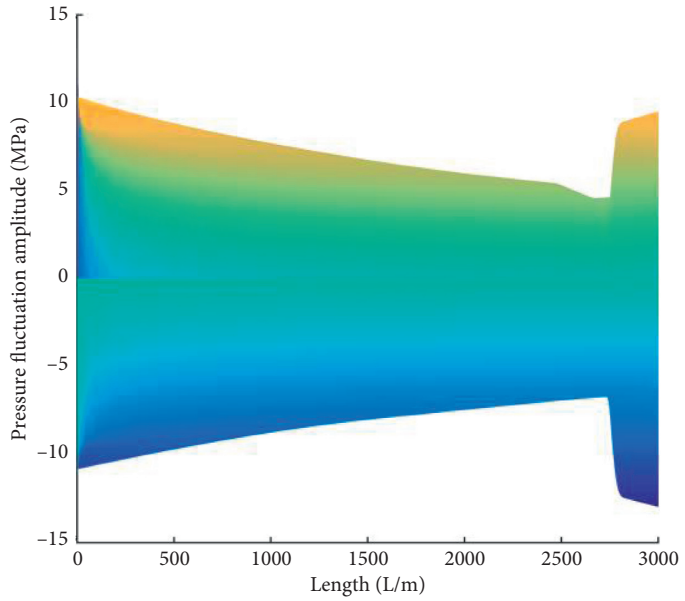

Figure 10: Comparison of pressure wave amplitude at different pipe string lengths.

compression effect. In this simulation, the maximum horizontal principal stress is set as horizontal direction, and the minimum horizontal principal stress is vertical direction. The circumferential stress in the horizontal direction of the inner wall of the wellbore is obviously greater than that in other directions. Therefore, the hydraulic fracture will initiate in this direction.

Figure 12 shows the simulation results of the variation of maximum circumferential stress on the inner wall of wellbore with injection time. Figure 12(a) shows the calculation result under the conventional stable injection scheme. It can be seen that at the initial stage of liquid injection, the circumferential stress of the inner wall is negative, showing compression effect. At this time, the bottom hole pressure is only the sum of the initial wellhead pressure and the gravity of the hydrostatic column in the string, which is not enough to overcome the influence of in situ stress. With the continuous injection of fracturing fluid, the bottom hole pressure gradually increases and the circumferential stress at the inner wall gradually raises. When the stop injection time t_2 is 17.1925 s, the circumferential stress at the inner wall is only 3.4060 MPa. This value is far lower than the tensile strength of the rock 8 MPa, which is not enough to make the reservoir to produce hydraulic fractures. In contrast,

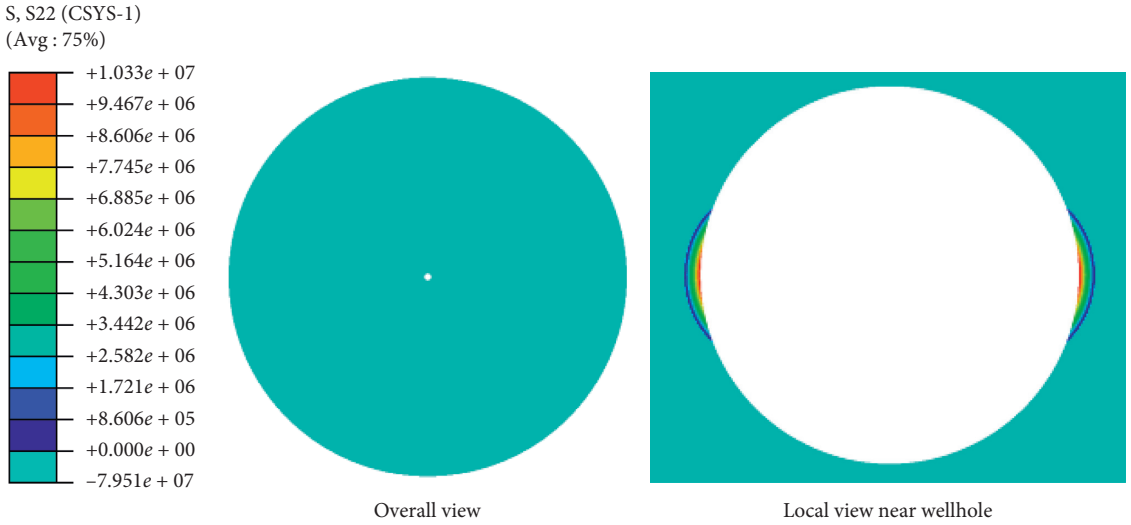

Figure 11: Distribution of circumferential stress in reservoir.

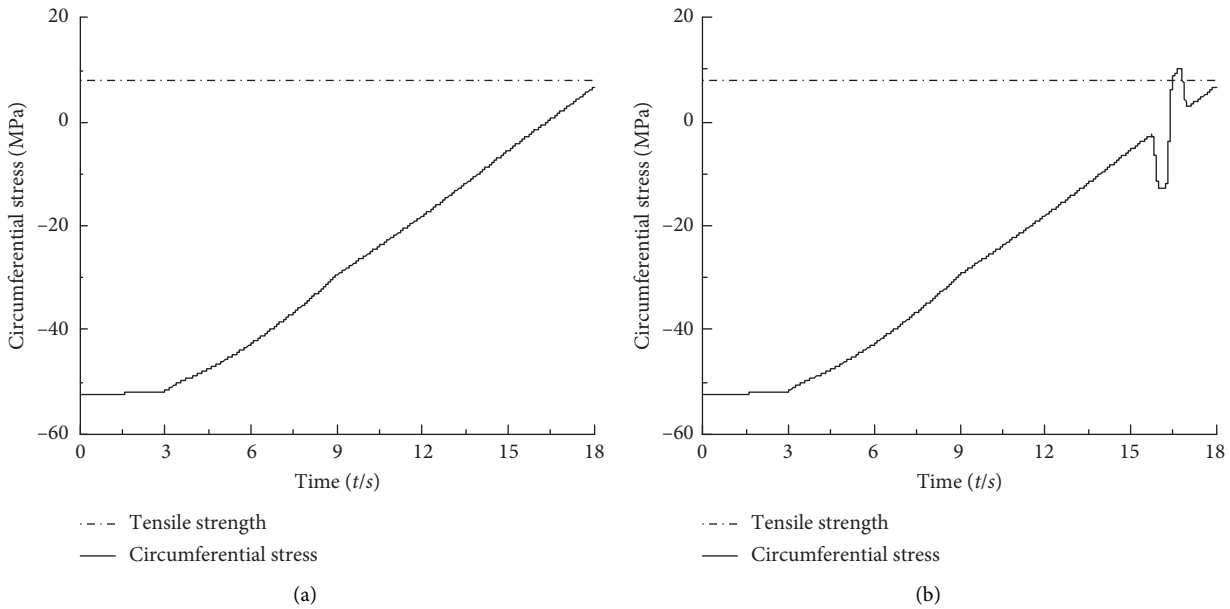

Figure 12: Comparison of circumferential stress variation of the wellbore inner wall with injection time. (a) Stable fluid-injection scheme. (b) Pulse fluid-injection scheme.

the simulation results of the pulse fluid injection are shown in Figure 12(b). The maximum circumferential stress of the inner wall of the wellbore can reach 10.3312 MPa. This method can effectively solve the problem that the breakdown pressure cannot be provided due to the safety pressure limit of surface equipment in the conventional stable liquid-injection scheme.

6.3. Parameter Analysis of Pulse Fluid-Injection Scheme. In the pulse fluid-injection scheme, the adjustment time t_1 and the adjustment amplitude ΔQ have significant influence on the fracturing effect. The above two factors will be discussed and analyzed in this section. From the previous simulation results, it can be seen that the pulse fluid injection will produce pressure wave. The pressure wave excites the reservoir and generates fluctuating dynamic stress in it. Thus, it is conducive to breaking the rock and forming a complex crack network. The fluctuation amplitude of dynamic stress in the reservoir is selected as the evaluation index of fracturing effect. Besides, the increase amplitude of stress is selected as another evaluation index of fracturing effect, which is the comparison result of pulse fluid injection with conventional stable fracturing.

6.3.1. Comparison of Pulse Adjustment Time. Taking the pulse adjustment time t_1 as the variable, the calculation results of fluctuation amplitude and increase amplitude of dynamic stress in reservoir are shown in Figure 13. It can be

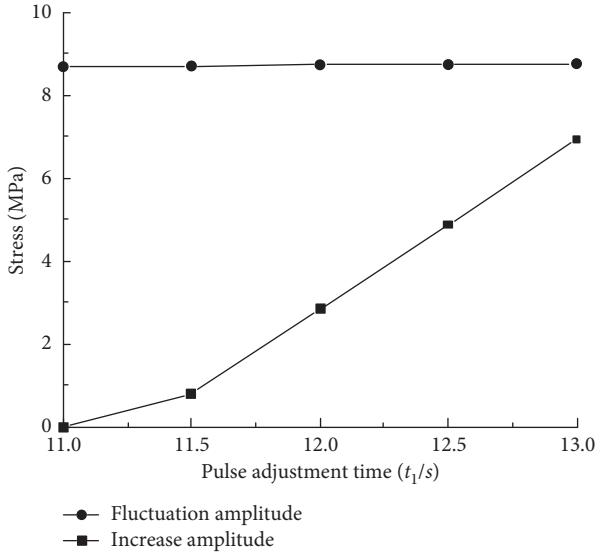

Figure 13: Influence of pulse adjustment time on dynamic stress in reservoir.

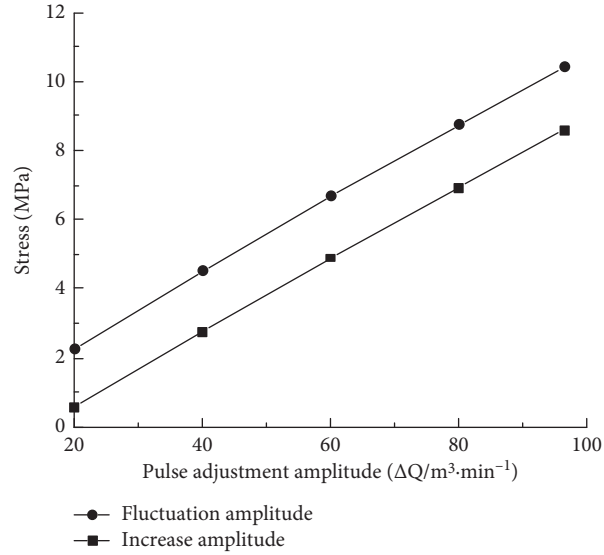

Figure 14: Influence of pulse adjustment amplitude on dynamic stress in reservoir.

seen that the fluctuation amplitude of dynamic stress is basically the same, while the increase amplitude raises with the increase in t_1. From the propagation characteristics of the pressure wave along the pipe string, it only affects the time when the pressure wave reaches the bottom of the well. Premature pulse injection adjustment makes the pressure wave reach the bottom of the well ahead of time. At this time, the bottom hole stable pressure value is small, and the superposition of them cannot effectively increase the bottom hole pressure. In other words, this pulse injection cannot effectively increase the circumferential stress of the inner wall of the wellbore. In contrast, when the pulse adjustment time is late, the stable pressure of the wellhead is close to the safe pressure. The wellhead pressure will exceed the safe pressure limit when the pulse adjustment is performed. At this time, pulse adjustment of wellhead pressure will easily exceed the safety pressure limit. Therefore, when other parameters in the pulse fluid-injection scheme have been determined, in order to maximize the increase amplitude of dynamic stress, the adjustment time t_1 needs to be optimized.

6.3.2. Comparison of Pulse Adjustment Amplitude. This section only discusses the influence of pulse adjustment amplitude on the fluctuation amplitude and the increase amplitude of dynamic stress in the reservoir. In the simulation, the amplitude of decreasing and increasing in pulse fluid-injection scheme is both ΔQ. The parameter ΔQ is the variation amplitude based on the stable injection flow Q_0. The simulation results are shown in Figure 14. It can be seen that with the increase in ΔQ, both the fluctuation amplitude and the increase amplitude of dynamic stress will also raise. When ΔQ is 96.5% of Q_0, the fluctuation amplitude and increase amplitude will reach the maximum. Once ΔQ exceeds 96.5% of Q_0, the wellhead pressure will exceed the safety pressure limit. That is to say, when the pulse adjustment time t_1 is determined, there is a maximum value of the adjustment amplitude of the injection flow. Under the condition that the safety pressure is not exceeded, increasing the adjustment amplitude ΔQ of pulse fluid injection is beneficial to raise the fluctuation amplitude and increase amplitude of dynamic stress in the reservoir.

7. Conclusion

To study the mechanism of pulse injection and give theoretical guidance in application, the transient flow model of fluid in the pipe string and the reservoir elastic dynamics model were, respectively, established in this paper. The adjustment parameters in the pulse injection scheme were also discussed. The main conclusions are as follows:

(1) The pulse injection scheme can effectively improve the bottom hole pressure and the internal stress of the reservoir. It is helpful to solve the practical problem that the breakdown pressure of reservoir cannot be provided due to the limitation of wellhead safety pressure. Moreover, the fluctuating fluid pressure further stimulates the reservoir to generate dynamic stress inside it.

(2) The principle of pulse fluid injection is that the unstable fluid-injection mode generates pulse pressure waves at the wellhead. Subsequently, the pressure wave propagates downward along the pipe string, and its amplitude attenuates due to the loss of resistance. This pressure wave is reflected after propagating to the bottom of the well, producing a reflected wave propagating upward. There is a superposition area of the downward pressure wave and upward reflection wave near the bottom hole. The bottom hole fluid pressure of pulse injection is the sum of stable injection pressure and the above pressure wave.

(3) The adjustment time and adjustment amplitude of the pulse injection scheme have an obvious influence on the fracturing effect. Although premature adjustment time can obtain dynamic stress in the reservoir, it cannot effectively increase the internal stress. Once the adjustment time is determined, the adjustment amplitude has a maximum value. In other words, without exceeding the safety pressure, increasing the adjustment amplitude is beneficial to improve the fracturing effect.

This study provides a theoretical basis for the application of pulse injection. In the future, the dynamic stress in the reservoir will be taken as the objective function to optimize the parameters of the pulse adjustment scheme.

Data Availability

The data used to support the findings of this study are available from the corresponding author upon request.

Conflicts of Interest

The authors declare that they have no conflicts of interest regarding the publication of this paper.

Acknowledgments

This study was supported by the National Natural Science Foundation of China (Grant no. 51974276) and Postgraduate Innovation Funding Project of Hebei Province (Grant no. CXZZBS2020052).

References

[1] D. J. Soeder, "The successful development of gas and oil resources from shales in North America," *Journal of Petroleum Science and Engineering*, vol. 163, pp. 399–420, 2018.

[2] W. Ma, Y. Wang, X. Wu, and G. Liu, "Hot dry rock (HDR) hydraulic fracturing propagation and impact factors assessment via sensitivity indicator," *Renewable Energy*, vol. 146, pp. 2716–2723, 2020.

[3] A. Josifovic, J. J. Roberts, J. Corney, B. Davies, and Z. K. Shipton, "Reducing the environmental impact of hydraulic fracturing through design optimisation of positive displacement pumps," *Energy*, vol. 115, pp. 1216–1233, 2016.

[4] R. House, M. Pry, and J. Pitcher, "The valve of pressure relief in hydraulic fracturing operations," in *Proceedings of the Texas USA: SPE Offshore Technology Conference*, Houston, Tx, USA, May 2017.

[5] L. Zhuang, S. G. Jung, M. Diaz et al., "Laboratory true triaxial hydraulic fracturing of granite under six fluid injection schemes and grain-scale fracture observations," *Rock Mechanics and Rock Engineering*, 2020.

[6] L. Zhuang, K. Y. Kim, S. G. Jung et al., "Cyclic hydraulic fracturing of pocheon granite cores and its impact on breakdown pressure, acoustic emission amplitudes and injectivity," *International Journal of Rock Mechanics and Mining Sciences*, vol. 122, pp. 1–9, 2019.

[7] S. M. Patel, C. H. Sondergeld, and C. S. Rai, "Laboratory studies of hydraulic fracturing by cyclic injection," *International Journal of Rock Mechanics and Mining Sciences*, vol. 95, pp. 8–15, 2017.

[8] Z. Zhou, G. Zhang, Y. Xing, Z. Y. Fan, X. Zhang, and D. Kasperczyk, "A laboratory study of multiple fracture initiation from perforation clusters by cyclic pumping," *Rock Mechanics and Rock Engineering*, vol. 52, no. 3, pp. 827–840, 2019.

[9] H. Bing, Z. Ruxin, T Peng et al., "Characteristics of fracture propagation in compact limestone formation by hydraulic fracturing in central Sichuan, China," *Journal of Natural Gas Science and Engineering*, vol. 57, pp. 122–134, 2018.

[10] J. Xie, J. Xie, G. Ni, R. Sheik, Q. Sun, and H. Wang, "Effects of pulse wave on the variation of coal pore structure in pulsating hydraulic fracturing process of coal seam," *Fuel*, vol. 264, pp. 1–10, 2020.

[11] J. Chen, X. Li, H. Cao, and L. Huang, "Experimental investigation of the influence of pulsating hydraulic fracturing on pre-existing fractures propagation in coal," *Journal of Petroleum Science and Engineering*, vol. 189, pp. 1–15, 2020.

[12] C. Jordan, M. Debotyam, and S. Iraj, "Variable pump rate fracturing leads to improved production in the marcellus shale," in *Proceedings of the Texas USA: SPE Hydraulic Fracturing Technology Conference*, The Woodlands, TX, USA, February 2016.

[13] J. Xu, C. Zhai, and L. Qin, "Mechanism and application of pulse hydraulic fracturing in improving drainage of coalbed methane," *Journal of Natural Gas Science and Engineering*, vol. 40, pp. 79–90, 2017.

[14] G. Ni, H. Xie, Z. Li, L. Zhuansun, and Y. Niu, "Improving the permeability of coal seam with pulsating hydraulic fracturing technique: a case study in Changping coal mine, China," *Process Safety and Environmental Protection*, vol. 117, pp. 565–572, 2018.

[15] P. Lu, G. Li, Z. Huang, Z. He, X. Li, and H. Zhang, "Modeling and parameters analysis on a pulsating hydro-fracturing stress disturbance in a coal seam," *Journal of Natural Gas Science and Engineering*, vol. 26, pp. 253–263, 2015.

[16] J. S. Yoon, G. Zimmermann, and A. Zang, "Numerical investigation on stress shadowing in fluid injection-induced fracture propagation in naturally fractured geothermal reservoirs," *Rock Mechanics and Rock Engineering*, vol. 48, no. 4, pp. 1439–1454, 2015.

[17] S. Tong, E. Gao, Y. Feng et al., "Mechanical principles of hydraulic pressure vibration method for improving hydraulic fracturing treatments-a new approach," in *Proceedings of the Washington USA: the 52nd US Rock Mechanics/Geomechanics Symposium*, Seattle, WA, USA, June 2018.

[18] W. Han, G. Zhou, Q. Zhang, H. Pan, and D. Liu, "Experimental study on modification of physicochemical characteristics of acidified coal by surfactants and ionic liquids," *Fuel*, vol. 266, pp. 1–12, 2020.

[19] A. Bergant, A. R. Simpson, and J. Vitkovsky, "Developments in unsteady pipe flow friction modeling," *Journal of Hydraulic Research*, vol. 39, pp. 249–257, 2001.

[20] J. P. Vitkovsky, M. F. Lambert, A. R. Simpson, and A. Bergant, "Advancesin unsteady friction modelling in transient pipe flow," in *Proceedings of the Hague Netherlands: the 8th International Conference on Pressure Surges*, The Hague, The Netherlands, April 2000.

[21] T. Liang, Z. Yang, F. Zhou et al., "A new approach to predict field-scale performance of friction reducer based on laboratory measurements," *Journal of Petroleum Science and Engineering*, vol. 159, pp. 927–933, 2017.

[22] S. Henclik, "Numerical modeling of water hammer with fluid-structure interaction in a pipeline with viscoelastic supports," *Journal of Fluids and Structures*, vol. 76, pp. 469–487, 2018.

[23] J. Hu, L. Wang, J. Feng, J. Shen, and M. He, "Full-life-cycle analysis of cement sheath integrity," *Mathematical Problems in Engineering*, vol. 2019, Article ID 8279435, 11 pages, 2019.

[24] K. H. S. M. Sampath, M. S. A. Perera, and P. G. Ranjith, "Theoretical overview of hydraulic fracturing break-down pressure," *Journal of Natural Gas Science and Engineering*, vol. 58, pp. 251–265, 2018.

[25] C. Yan, J. Deng, L. Hu, and B. Yu, "Fracturing pressure of shallow sediment in deep water drilling," *Mathematical Problems in Engineering*, vol. 2013, Article ID 492087, 8 pages, 2013.